JACS
JOURNAL OF THE AMERICAN CHEMICAL SOCIETY

ARTICLE

pubs.acs.org/JACS

Mimicking the Role of the Antenna in Photosynthetic Photoprotection

Yuichi Terazono,[†] Gerdenis Kodis,[†] Kul Bhushan,[†] Julia Zaks,[‡,§] Christopher Madden,[†] Ana L. Moore,[*,†] Thomas A. Moore,[*,†] Graham R. Fleming,[*,§,⊥] and Devens Gust[*,†]

[†]Department of Chemistry and Biochemistry, Center for Bioenergy and Photosynthesis, and Center for Bio-Inspired Solar Fuel Production, Arizona State University, Tempe, Arizona 85287, United States

[‡]Applied Science and Technology Graduate Group, University of California, Berkeley, Berkeley, California 94720, United States

[§]Physical Biosciences Division, Lawrence Berkeley National Laboratory, Berkeley, California 94720, United States

[⊥]Department of Chemistry and QB3 Institute, University of California, Berkeley, Berkeley, California 94720, United States

Supporting Information

ABSTRACT: One mechanism used by plants to protect against damage from excess sunlight is called nonphotochemical quenching (NPQ). Triggered by low pH in the thylakoid lumen, NPQ leads to conversion of excess excitation energy in the antenna system to heat before it can initiate production of harmful chemical species by photosynthetic reaction centers. Here we report a synthetic hexad molecule that functionally mimics the role of the antenna in NPQ. When the hexad is dissolved in an organic solvent, five zinc porphyrin antenna moieties absorb light, exchange excitation energy, and ultimately decay by normal photophysical processes. Their excited-state lifetimes are long enough to permit harvesting of the excitation energy for photoinduced charge separation or other work. However, when acid is added, a pH-sensitive dye moiety is converted to a form that rapidly quenches the first excited singlet states of all five porphyrins, converting the excitation energy to heat and rendering the porphyrins kinetically incompetent to readily perform useful photochemistry.

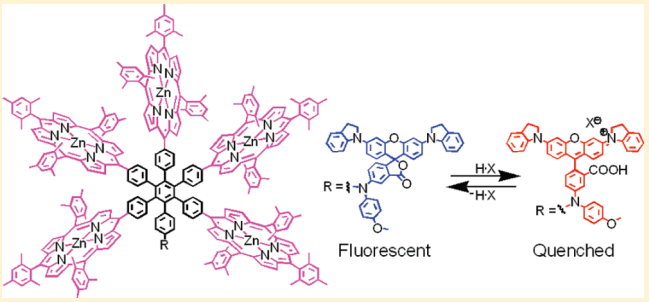

INTRODUCTION

Most of the sunlight used by plants to make fuels through photosynthesis is harvested by antennas. These chromophore arrays, excellent examples of natural nanotechnology, transfer excitation energy to reaction centers where it is converted to electrochemical potential energy via photoinduced electron transfer. The electrochemical energy is used in subsequent "dark" reactions including the synthesis of ATP and of reducing equivalents that are employed to prepare carbohydrate and other fuels. Under intense sunlight, the reactive redox intermediates produced by reaction centers are generated more rapidly than they can be used by the dark reactions. The excess reactive species can cause tissue damage or generate toxins such as singlet oxygen. One way that plants protect themselves against such harm is nonphotochemical quenching (NPQ), a process whereby excess excitation in the antenna is degraded to heat, preventing the generation of surplus redox capacity.[1−5]

NPQ is triggered by chemistry initiated in the reaction centers. Electron transfer in reaction centers releases protons into the thylakoid lumen, leading to a pH and charge gradient across the photosynthetic membrane. Chemical potential stored in this gradient powers many of the subsequent reactions of energy conversion. At high light levels the lumen pH drops, signaling that electron transfer is outpacing the fuel-producing reactions that consume the pH gradient. Low pH activates NPQ, wherein changes in the antenna system regulate reaction center function by diverting excitation energy into heat before it can be transferred to the reaction centers and initiate electron transfer. The process by which this occurs is not fully understood but in some organisms is known to involve protonation of two residues on a protein known as PsbS and chemical modification of a carotenoid polyene. The modified polyene quenches antenna chlorophyll excited states, possibly by electron and/or energy transfer.[3,6−11]

Although humans are becoming adept at designing molecules to perform catalytic or other functions, examples of such molecules that can also regulate their function in response to external stimuli are rare. Here, we report molecular hexad **1** (Figure 1) that functionally mimics the role of the antenna in NPQ. The molecule features five porphyrin antenna moieties and a pH-sensitive dye, comprising a model multichromophoric photosynthetic antenna coupled to a control unit. Under neutral conditions, the porphyrins rapidly exchange excitation energy and have long-lived excited states capable of doing photochemical work. When the solution is made acidic, the dye moiety is converted to a form that quenches the first excited singlet states of all five porphyrins on the picosecond time scale, rendering them kinetically incompetent to carry out additional photochemistry and converting the excitation energy to heat. In addition to providing a simple functional model for the antenna in NPQ, the hexad

Received: August 27, 2010
Published: February 11, 2011

dx.doi.org/10.1021/ja107753f | J. Am. Chem. Soc. 2011, 133, 2916–2922

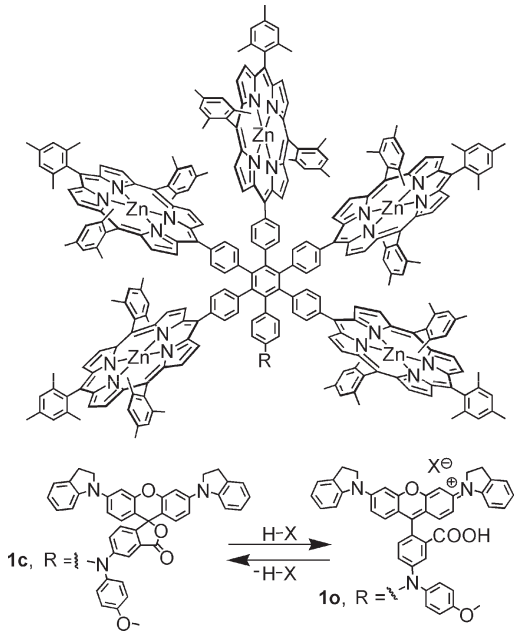

Figure 1. Structures of the hexads. Hexad **1o** is generated from closed form **1c** upon treatment with an acid, H−X, where X represents the conjugate base.

demonstrates the kind of self-regulatory behavior that will be needed if the promise of nanotechnology is to be fully realized.[12]

RESULTS

Synthesis. The five zinc porphyrin moieties that comprise the antenna portion of hexad **1** are covalently linked to a hexaphenylbenzene core at porphyrin meso positions. The hexaphenylbenzene also bears a rhodamine-type pH-sensitive dye, and serves as a relatively rigid framework that controls electronic interactions among the attached chromophores. Under neutral conditions, the hexad exists with the dye in the spirocyclic form **1c**, but when the medium becomes sufficiently acidic, the molecule is protonated and converted to **1o**, in which the dye is in the open, positively charged form. The synthesis and characterization of hexad **1** and model compounds **2**−**4** (Figure 2) are detailed in the Supporting Information. The general outline of the synthetic route to **1** is as follows. The basic hexaphenylbenzene skeleton was prepared by a variation of the cyclotrimerization method of Takase, et al.[13] Two acetylene moieties, each bearing two nickel porphyrins, and a third acetylene bearing a nickel porphyrin and a substituted aniline were cyclized using a dicobalt octacarbonyl catalyst. After removal of the nickel with sulfuric acid and insertion of zinc into the porphyrins, the resulting hexaphenylbenzene precursor bearing five zinc porphyrins was coupled to the dye precursor via a palladium-catalyzed amination. The pH-sensitive dye precursor was synthesized on the basis of a method reported by Woodroofe, et al.[14] for related compounds. Models **2**, **3**, and **4** were synthesized using similar methods. New compounds were characterized by mass spectrometry, ^{1}H NMR, and UV−vis spectroscopy.

Absorption and Fluorescence Spectra. The absorption spectrum of **1c** in dichloromethane is shown in Figure 3a. It features the porphyrin Soret (B) at 423 nm and Q-bands at 514, 551, and 590 nm. The dye portion of the molecule does not absorb in the visible spectral region but has bands at 309 and 336 nm. As

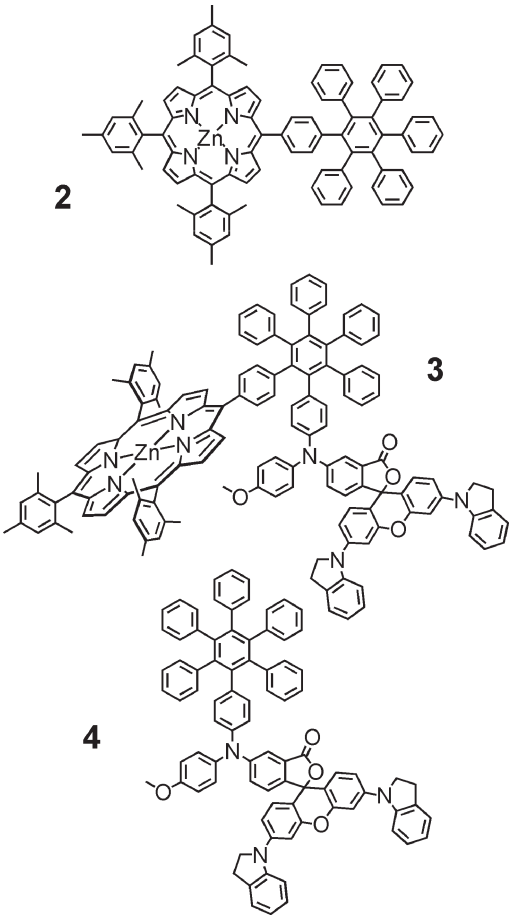

Figure 2. Structures of model compounds. In model dyad **3** and model dye **4** the dye moiety is shown only in the closed, spirocyclic form. The open form is analogous to that shown in Figure 1.

shown in Figure 4, the Soret band of **1c** is broader (see shoulder at ∼408 nm) and slightly shifted to longer wavelengths relative to that of model compound **2** comprising a single zinc porphyrin (Figure 2), indicating excitonic interactions among adjacent porphyrin moieties. Excitonic interactions of this type have been observed in similar compounds,[15−17] including a closely related porphyrin array, and the nature of the interactions discussed in some detail.[18] The Q-band shapes and wavelengths are essentially identical to those in **2**. As acetic acid is added, portion-wise, to the solution of **1**, a new absorbance with a maximum at 656 nm grows in (Figure 3a). The new band is characteristic of the open form of the dye, signaling conversion of **1c** to **1o** by protonation. The zinc porphyrin spectral features are unchanged upon addition of acetic acid, indicating that zinc is not removed from the porphyrins by the acid.

The conversion of **1c** to **1o** is accompanied by profound changes in the porphyrin fluorescence emission (Figure 3b). Hexad **1c** shows typical zinc porphyrin emission at 602 and 650 nm. As acid is added to the solution, the shape of the emission is unchanged, but the emission intensity decreases substantially. The decrease indicates that in the open form of the dye, which predominates in the solution, emission from all five porphyrin moieties is strongly quenched. Treatment of acidified solutions of **1** with sodium carbonate to neutralize the acid results in recovery of the original absorption and emission spectra (Figure 3). Thus, the protonation is reversible, and the ratio of **1o** to **1c** in the solution is a function of the amount of acid added.

dx.doi.org/10.1021/ja107753f |*J. Am. Chem. Soc.* 2011, 133, 2916–2922

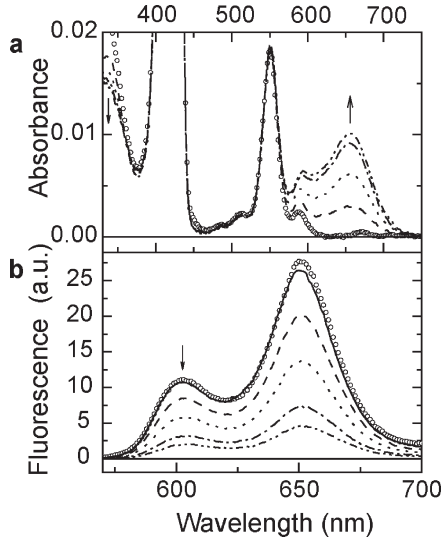

Figure 3. Absorption and emission spectra of the hexads. (a) Absorption spectra of **1c** in dichloromethane (solid) and after addition of acetic acid, which converts some of the **1c** to **1o**: acetic acid at 123 mM (dash), 244 mM (dot), 482 mM (dash−dot), and 826 mM (dash−dot−dot). (b) Fluorescence emission spectra (λ_{ex} = 396 nm) of the solutions described in (a). The spectral amplitudes in (a) and (b) have been corrected for dilution by acid. After completion of these measurements, the acetic acid was removed by treating the solution with excess granular sodium carbonate and filtering. The absorption and emission spectra of the resulting solution are shown (circles). This treatment led to the reversion of **1o** to **1c**. It also caused the appearance of a very small absorption at 670 nm, and a small emission band (not shown) at ∼720 nm. These features are ascribed to a small amount of impurity or decomposition appearing after the neutralization process.

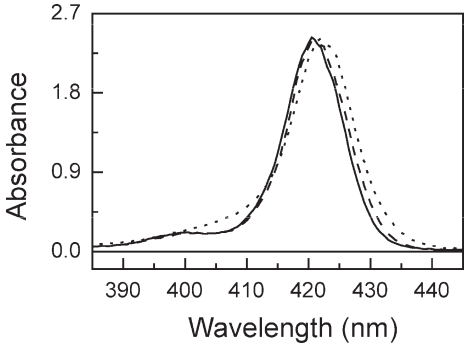

Figure 4. Absorption spectra in the Soret region of dichloromethane solutions of model porphyrin **2** (solid), porphyrin-dye dyad **3** with the dye in the closed, spiro form (dash), and hexad **1c** with the dye in the closed, spiro form (dot). Note the broadening and slight shift of the hexad Soret band, which indicates excitonic interactions among the porphyrin moieties.

Transient Spectroscopy. Information about the quenching process was obtained from transient spectroscopy. Fluorescence emission data were obtained from two different spectrometers: a streak camera setup and a conventional single-photon timing apparatus. In each case, the decays were analyzed by least-squares fitting as a sum of exponentials, with reconvolution to remove effects from the instrument response as described in the Experimental Section. Both apparatus produced reliable time constants down to ∼5 ps, with the goodness of fit (χ^2) values reported below.

Fluorescence emission studies with the streak camera (Figure 5) showed that when a dichloromethane solution of **1c** was excited at

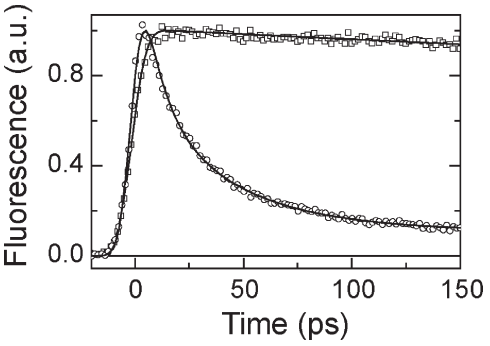

Figure 5. Emission decays for **1** at 650 nm following excitation at 550 nm with a 130 fs laser pulse. Decays were obtained from **1c** in dichloromethane (squares) and from an acidified solution highly enriched in **1o** (circles). The solid lines are best fits to exponential functions with time constants as described in the text.

550 nm, where the light is absorbed by the porphyrin Q-bands, the decay of the fluorescence emission (monitored at 650 nm) could be fitted with a single exponential having a time constant of 2.14 ns (Figure 5, χ^2 = 1.16). Such a lifetime is typical of zinc porphyrins of this general type (vide infra).

The fluorescence decay of the solution of **1** was measured again (Figure 5) after addition of acetic acid, which converted most of the sample to **1o**. The decay was fitted (χ^2 = 1.21) with exponential components having time constants of 10.3 ps (49%), 39.4 ps (31%), and 2.10 ns (20%). The 2.1 ns contribution is due to residual **1c**, and the picosecond components represent drastic reduction of the porphyrin first excited singlet state lifetimes; for **1o**, the rate constants of the quenching processes are 9.7×10^{10} s^{-1} and 2.5×10^{10} s^{-1}. The quantum yield of fluorescence quenching is essentially unity, as calculated on the basis of either of the two picosecond time constants and the lifetime of **1c**.

In order to better understand the nature of the quenching process in **1o**, we prepared and studied a model dyad **3** (Figure 2), which consists of a pH-sensitive dye identical to that in **1** linked to a hexaphenylbenzene core that features a single zinc porphyrin at a position ortho to the dye. The dyad with the dye in the closed, spirocyclic form, dissolved in dichloromethane, showed Soret and Q-band absorption maxima and fluorescence maxima at wavelengths similar to those observed for **2**. Time-resolved fluorescence experiments using the single-photon timing method with excitation at 425 nm and emission at 600 nm yielded a lifetime for the porphyrin first excited singlet state of 2.09 ns (Figure 6). The fluorescence of model porphyrin **2**, measured using the same apparatus, decayed as a single exponential with a lifetime of 2.13 ns (not shown, χ^2 = 1.02).

Addition of acetic acid to the solution of **3** converted most of the dyad to the open, protonated form, which had a porphyrin first excited singlet state lifetime, measured using single-photon timing, of 23 ps (Figure 6). This time constant represents quenching of the first excited singlet state of the porphyrin by the open form of the adjacent dye.

Turning again to the hexad, we associate the 10-ps decay observed for **1o** mainly with quenching of the two porphyrins ortho to the dye by the dye moiety. The time constant is comparable to that measured for the similar process in **3** (23 ps), given the fact that the two molecules are not identical. In the hexad, the porphyrins next to the dye moiety experience strong steric interactions with it and the adjacent porphyrins (not present in dyad **3**), and these result in conformational changes that undoubtedly

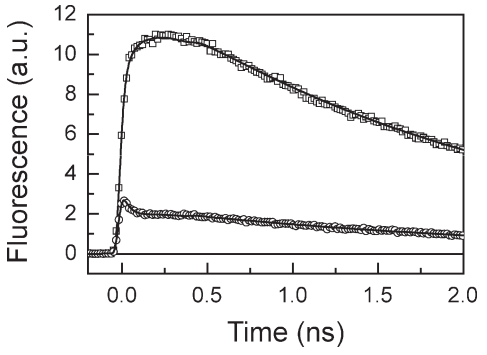

Figure 6. Fluorescence emission decays at 600 nm following excitation at 425 nm of a solution of dyad **3** in 2.5 mL of dichloromethane. The squares indicate the data for the dyad in the closed, spirocyclic form, and the accompanying solid line is a best exponential fit to the data that yields lifetimes of 2.09 ns (99.3%) and 8.2 ns (0.7%), with $\chi^2 = 1.16$. The small amount of 8.2 ns decay is ascribed to the free base form of the porphyrin. The circles indicate data for the solution after addition of 250 μL of acetic acid, which converts most of the dyad to the open, protonated form. Exponential fitting gives time constants of 23 ps (70%) and 2.12 ns (30%), with $\chi^2 = 1.13$. The shorter time constant is associated with the protonated form of the dyad, and the longer time constant with the closed, spirocyclic form. The apparent rise at early times is due to the convolution of the decay kinetics with the instrument response function.

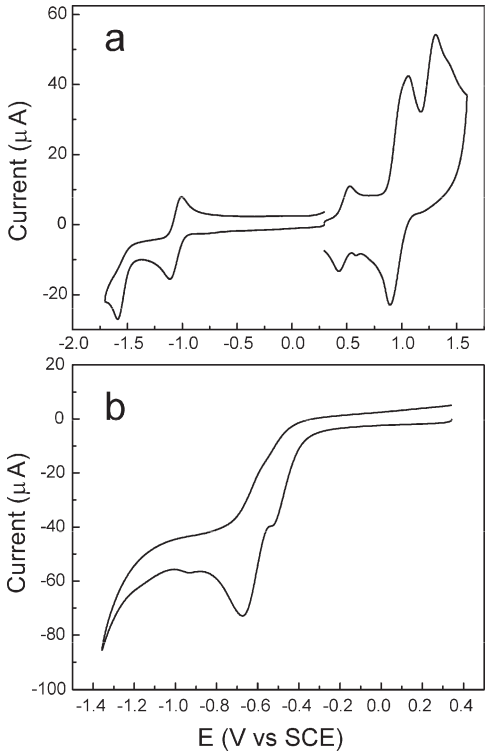

Figure 7. Cyclic voltammograms of (a) model dye **4** dissolved in dichloromethane containing 0.1 M tetra-*n*-butylammonium hexafluorophosphate and (b) the same solution after addition of sufficient acetic acid to convert most of the dye to the open, protonated form. The potentials were measured with ferrocene as an internal reference and are reported relative to SCE. The waves around 0.5 V are due to ferrocene.

alter the energy transfer time constants. The 39 ps decay must then result from some combination of direct quenching of the porphyrins meta and para to the dye by the dye moiety and singlet energy transfer among the porphyrins. In a detailed study of a porphyrin array with very similar, but not identical, porphyrin structures, a time constant for exchange of energy between adjacent porphyrins of ~180 ps was estimated from fluorescence anisotropy results.[18] If we assume that a similar time constant is appropriate for **1**, then it is clear that the rapid (~39 ps) transfer of excitation to the open dye from the porphyrin moieties meta and para to it must involve energy transfer directly from these porphyrins to the dye moiety. In principle, the kinetics for direct transfer will be convoluted to some extent with excitation hopping between porphyrins. However, kinetic simulations reveal that if we assume that meta and para transfer both occur with time constants of 39 ps and ortho transfer occurs with a time constant of 10 ps, inclusion of the time constant for exchange of energy between porphyrins has a negligible effect on the porphyrin first excited singlet state decay profile. The time constants for energy transfer involving the porphyrins in the meta and para locations are undoubtedly different from one another, but extraction of additional time constants was not justified by data analysis. It is clearly evident that the dye in its open, protonated form rapidly quenches the excited singlet states of all five porphyrins.

Model dye **4** (Figure 2) in its protonated form did not show measurable fluorescence when studied by single-photon timing methods. Therefore, the excited singlet state lifetime was measured in ethanol with excitation at 640 nm using femtosecond transient absorption spectroscopy. Figure 8 shows excited-state relaxation to the ground state (decay of ground-state bleaching at 640 nm) and an exponential least-squares fit with a time constant of 5.0 ps.

Quenching Mechanism. Two possible mechanisms for quenching of the porphyrin excited states by the protonated form of the dye are singlet−singlet energy transfer to the dye, yielding an excited state of the dye, and photoinduced electron transfer yielding a charge-separated state. In order to investigate the thermodynamic requirements for quenching by photoinduced electron transfer, we measured the electrochemical properties of model dye **4** (Figure 2). The results of cyclic voltammetric experiments in dichloromethane containing 0.1 M tetra-*n*-butylammonium hexafluorophosphate are shown in Figure 7. The working electrode was glassy carbon, the counter electrode was platinum foil, and the reference electrode was a silver wire in 10 mM silver nitrate in acetonitrile containing the same electrolyte. The potentials were converted to the SCE scale using ferrocene as an internal reference compound.

Representative results for **4** in the closed, spirocyclic form are shown in Figure 7a. The first oxidation was observed at 0.94 V vs SCE, and the first reduction at −1.11 V vs SCE. Both waves were essentially reversible. The waves around 0.5 V are due to ferrocene. A representative voltammogram after addition of 80 μL of acetic acid in order to convert most of the dye to the open, protonated form is shown in Figure 7b. Although the voltammogram is not reversible, it is clear that reductive processes occur in the −0.5 to −0.6 V region.

On the basis of the oxidation potential of zinc tetramesitylporphyrin (0.68 V vs SCE[19]) and the reduction behavior of model dye **4**, quenching via photoinduced electron transfer from the excited porphyrin to the protonated dye is thermodynamically possible. However, electron transfer requires overlap of donor and acceptor molecular orbitals, which is expected to be rather weak in **1o**, given the large number of bonds between the porphyrins and dye moiety ortho, meta, and para to them and the fact that steric hindrance at the center of the hexaphenylbenzene

dx.doi.org/10.1021/ja107753f |*J. Am. Chem. Soc.* 2011, 133, 2916–2922

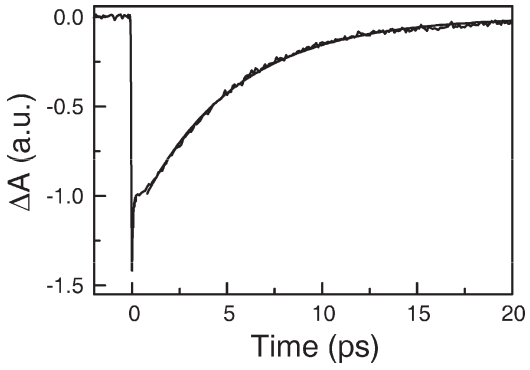

Figure 8. Transient absorption at 640 nm (arbitrary units) of an ethanol solution of model dye **4** excited with a 54-fs laser pulse at 640 nm. The solution contained sufficient formic acid to convert the molecule to its open, protonated form. The data show the decay of the dye ground-state bleach as the first excited singlet state returns to the ground state. The smooth curve is an exponential fit to the decay with a time constant of 5.0 ps. The χ^2 value (unreduced) is 0.16. The initial part of the decay is convoluted with coherence artifacts arising from cross-phase modulation, and were omitted from the data fitting.

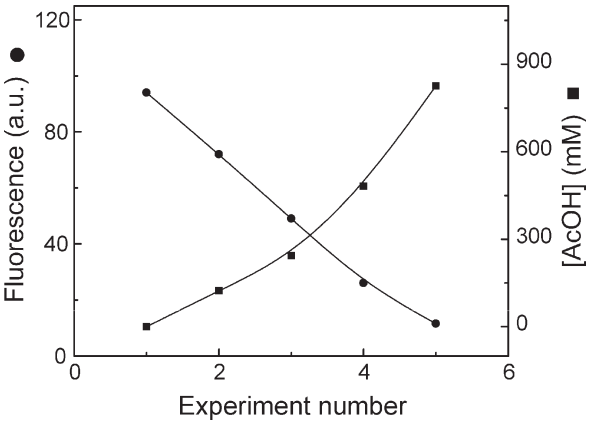

Figure 9. Hexad **1** fluorescence quenching upon addition of acid. A solution of **1** in dichloromethane was prepared, and the zinc porphyrin fluorescence intensity at 650 nm (circles) was monitored as the acetic acid concentration (squares) was increased. The fluorescence data have been corrected for dilution of the solution by the added acid.

core leads to near-orthogonality of the central and peripheral benzene rings.[20−22]

Singlet−singlet energy transfer, on the other hand, usually occurs by the Coulombic (Förster) mechanism,[23] which does not require orbital overlap and depends in part on interchromophore separation and orientation. In **1o**, the spatial proximity of the dye moiety and the zinc porphyrins is favorable for singlet−singlet energy transfer, as is the energy overlap of porphyrin emission and dye absorption. Rate constants for singlet−singlet energy transfer from porphyrin moieties of **1o** to the dye moiety in the open, protonated form were calculated using the Förster theory. In these calculations, the transition dipole moment for the protonated dye molecule was assumed to lie in the same position as it does in the related rhodamine 6G.[24] The fluorescence quantum yield for the zinc porphyrins in the absence of energy transfer was taken as 0.04.[25] The extinction coefficient for the dye in the open form at 656 nm was measured as 5.7×10^4 M^{-1} cm^{-1} for model dye **4**. Modeling using molecular mechanics (MM2) showed that several conformations for the dye relative to the porphyrin moieties were likely. For the porphyrin para to the dye, distances between the transition dipoles ranged from 20.9 Å to 21.5 Å. Assuming an orientation factor κ^2 equal to 2/3 (random orientation), these distances gave energy transfer time constants of 40.6 and 48.1 ps, respectively. Energetically reasonable conformations for the molecule featured distances between the dipoles of the dye and a porphyrin ortho to it, ranging between 12.5 Å and 15.3 Å. A κ^2 of 2/3 yielded time constants of 1.9 and 6.25 ps for these separations. Transfer rates between the open dye and a porphyrin meta to it were not calculated, but would lie between those for the ortho and para porphyrins.

The calculated time constants for energy transfer from a porphyrin to a dye moiety ortho and para to it are relatively close to the measured lifetimes of 10 and 39 ps. Thus, the quenching in **1o** is consistent with energy transfer from porphyrin to the protonated dye. Assignment of the quenching to energy transfer is strongly supported by the observation that the time constants for decay of the zinc porphyrin excited states of **1o** in ethanol (9 and 39 ps) are nearly identical to those in dichloromethane. The dielectric constant of ethanol (24) is significantly larger than that of dichloromethane (9), and electron transfer rates are strongly dependent on solvent polarity, which affects both reorganization energies and driving force. Energy transfer is generally not a strong function of solvent polarity. Direct observation of energy transfer by transient spectroscopy in **1o** would be difficult because the lifetime of the first excited singlet state of model dye **4** in its protonated form, measured in ethanol by transient absorption spectroscopy, is only 5 ps (Figure 8), which is shorter than the time constants of the processes that populate it.

■ DISCUSSION

It is clear from the above results that absorption of visible light by hexad **1c** results in the formation of zinc porphyrin excited singlet states that exchange excitation energy by singlet−singlet energy transfer. The ensemble of excited singlet states decays exponentially with a time constant of 2.1 ns, which is essentially the same lifetime as observed for related monomeric zinc porphyrin **2**. As has been shown by numerous studies,[26−28] such long-lived singlet states are ideal for driving photoinduced electron transfer which converts excitation energy to chemical potential. When a solution of **1** is acidified, protonation of the dye converts **1c** to **1o**, in which the porphyrin first excited singlet states are quenched to <40 ps, rendering them kinetically incompetent to readily donate electrons to useful acceptor moieties and ultimately converting the excitation energy to heat. The effect is shown graphically in Figure 9, where the porphyrin fluorescence at 650 nm is seen to decrease as the acid concentration increases. Each porphyrin moiety in the array is quenched by the protonated dye via a process ascribed to singlet−singlet energy transfer. The transfer rates are consistent with those calculated using simple Förster theory. The resulting excited dye moiety rapidly (5 ps) decays to the ground state. Thus, as the acidity of a solution of **1** is increased, the fraction of hexad molecules able to perform useful photochemistry decreases accordingly: the system down-regulates its photochemical efficiency as acidity increases. The hexad photochemistry thus mimics the antenna system function in the NPQ photoprotective process in green plants, where antenna chlorophyll excited-state quenching is triggered by decreasing pH in the thylakoid lumen. In addition to providing a model framework in which to investigate the principles underlying natural NPQ, the hexad shows that incorporation of self-regulation

of function in response to external stimuli is also possible in human-made nanosystems for solar energy conversion.

EXPERIMENTAL SECTION

The details for the synthesis and characterization of all new compounds reported are given in the Supporting Information. Spectroscopic studies were carried out on dilute ($\sim 10^{-5}$ M) solutions in dichloromethane, and acetic acid was added to convert the dye to the protonated form, unless otherwise specified. Random errors associated with the reported lifetimes were typically $\leq 5\%$.

Steady-State Spectroscopy. Absorption spectra were measured on a Shimadzu UV2100U UV−vis and/or UV-3101PC UV−vis−NIR spectrometer. Steady-state fluorescence spectra were measured using a Photon Technology International MP-1 spectrometer and corrected for detection system response. Excitation was provided by a 75 W xenon-arc lamp and single grating monochromator. Fluorescence was detected 90° to the excitation beam via a single grating monochromator and an R928 photomultiplier tube having S-20 spectral response and operating in the single-photon counting mode.

Time-Resolved Fluorescence. Fluorescence decay measurements were performed employing two different systems: a conventional single-photon timing apparatus and a streak camera setup. The excitation source for the single-photon timing system was a mode-locked Ti:Sapphire laser (Spectra Physics, Millennia-pumped Tsunami) with a 130-fs pulse duration operating at 80 MHz. The laser output was sent through a frequency doubler and pulse selector (Spectra Physics model 3980) to obtain 370−450 nm pulses at 4 MHz. Fluorescence emission was detected at the magic angle using a double grating monochromator (Jobin Yvon Gemini-180) and a microchannel plate photomultiplier tube (Hamamatsu R3809U-50). The instrument response function was 35−55 ps. The spectrometer was controlled by software based on the LabView programming language, and data acquisition was done using a single-photon counting card (Becker-Hickl, SPC-830).

Time vs wavelength fluorescence intensity surfaces were recorded on the streak camera system, with excitation provided by an ultrafast laser. Laser pulses of ~130 fs at 800 nm were generated from an amplified, mode-locked titanium-sapphire 250 kHz laser system (Verdi/Mira/RegA, Coherent). The excitation light wavelength was adjusted using an optical parametric amplifier (Coherent). Fluorescence with polarization set to the magic angle was collected 90° to the excitation beam and focused on the entrance slit of a Chromex 250IS spectrograph, which was coupled to a Hamamatsu C5680 streak camera with a M5675 synchroscan sweep unit. The streak images were recorded on a Hamamatsu C4742 CCD camera and curvature corrected (corrections for shading and system detection sensitivity at different wavelengths were not performed). The instrument response function was ~5−20 ps.

Data analysis of results from both systems was carried out using locally written software (ASUFIT) developed in a MATLAB environment (Mathworks Inc.). Data were fitted as a sum of exponential decays, which were reconvoluted with the appropriate instrument response function. Goodness of fit was established by examination of residuals and the reduced χ^2 value.

Transient Absorption Spectroscopy. Transient absorption spectroscopy was carried out by the pump−probe technique. The femtosecond light source was an optical parametric amplifier (Coherent OPA) pumped by a 250 kHz Ti:sapphire regenerative amplifier (Coherent RegA 9050) that was seeded by a Ti:sapphire oscillator (Coherent Mira Seed). The output of the OPA was tuned to 640 nm and compressed with prisms to 54 fs. These pulses were divided by a beam splitter, and the probe beam was attenuated with a neutral density filter to 20 μW. The pump beam was sent through an optical delay line, and the beams were crossed at the sample position. The power of the pump at the sample was 1 mW. The probe beam intensity was measured with a photodiode (Thorlabs DET 210) connected to a lock-in amplifier (Stanford Research Systems SR830) that was synchronized with a mechanical chopper modulating the pump path at 499 Hz. The observed kinetics were independent of both pump and probe intensity. The measured transient absorption signal was fit with a single exponential decay using least-squares analysis, and goodness of fit was established from residuals. The fitting was restricted to the part of the curve where the effects of the excitation pulse and coherence artifacts were negligible.

ASSOCIATED CONTENT

Supporting Information. Experimental details of the synthesis and characterization of the molecules described. This material is available free of charge via the Internet at http://pubs.acs.org.

AUTHOR INFORMATION

Corresponding Author
gust@asu.edu; GRFleming@lbl.gov

ACKNOWLEDGMENT

This work was funded by the Helios Solar Energy Research Center, which is supported by the Director, Office of Science, Office of Basic Energy Sciences of the U.S. Department of Energy under Contract No. DE-AC02-05CH11231. G.K. was supported as part of the Center for Bio-Inspired Solar Fuel Production, an Energy Frontier Research Center funded by the U.S. Department of Energy, Office of Science, Office of Basic Energy Sciences under Award Number DE-SC0001016. C.M. thanks the Science Foundation Arizona for financial support.

REFERENCES

(1) Demmig-Adams, B.; Adams, W. W., III. *Science* **2002**, *298*, 2149–2153.
(2) Berera, R.; van Stokkum, I. H. M.; d'Haene, S.; Kennis, J. T. M.; van Grondelle, R.; Dekker, J. P. *Biophys. J.* **2009**, *96*, 2261–2267.
(3) Ruban, A. V.; Berera, R.; Ilioaia, C.; van Stokkum, I. H. M.; Kennis, J. T. M.; Pascal, A. A.; van Amerongen, H.; Robert, B.; Horton, P.; van Grondelle, R. *Nature* **2007**, *450*, 575–578.
(4) Ahn, T. K.; Avenson, T. J.; Ballottari, M.; Cheng, Y. C.; Niyogi, K. K.; Bassi, R.; Fleming, G. R. *Science* **2008**, *320*, 794–797.
(5) Li, X. P.; Gilmore, A. M.; Caffarri, S.; Bassi, R.; Golan, T.; Kramer, D.; Niyogi, K. K. *J. Biol. Chem.* **2004**, *279*, 22866–22874.
(6) Horton, P.; Ruban, A. V. *J. Exp. Botany* **2005**, *56*, 365–373.
(7) Pascal, A. A.; Liu, Z. F.; Broess, K.; van Oort, B.; van Amerongen, H.; Wang, C.; Horton, P.; Robert, B.; Chang, W. R.; Ruban, A. *Nature* **2005**, *436*, 134–137.
(8) Holt, N. E.; Fleming, G. R.; Niyogi, K. K. *Biochemistry* **2004**, *43*, 8281–8289.
(9) Berera, R.; Herrero, C.; van Stokkum, L. H. M.; Vengris, M.; Kodis, G.; Palacios, R. E.; van Amerongen, H.; van Grondelle, R.; Gust, D.; Moore, T. A.; Moore, A. L.; Kennis, J. T. M. *Proc. Natl. Acad. Sci. U.S.A.* **2006**, *103*, 5343–5348.
(10) Kulheim, C.; Ågren, J.; Jansson, S. *Science* **2002**, *297*, 91–93.
(11) Wilson, A.; Punginelli, C.; Gall, A.; Bonetti, C.; Alexandre, M.; Routaboul, J. M.; Kerfeld, C. A.; van Grondelle, R.; Robert, B.; Kennis, J. T. M.; Kirilovsky, D. *Proc. Natl. Acad. Sci. U.S.A.* **2008**, *105*, 12075–12080.
(12) Stephanopoulos, N.; Solis, E. O. P.; Stephanopoulos, G. *AIChE J.* **2005**, *51*, 1858–1869.
(13) Takase, M.; Ismael, R.; Murakami, R.; Ikeda, M.; Kim, D.; Shinmori, H.; Furuta, H.; Osuka, A. *Tetrahedron Lett.* **2002**, *43*, 5157–5159.
(14) Woodroofe, C. C.; Lim, M. H.; Bu, W. M.; Lippard, S. J. *Tetrahedron* **2005**, *61*, 3097–3105.

(15) Liddell, P. A.; Kodis, G.; de la Garza, L.; Moore, A. L.; Moore, T. A.; Gust, D. *J. Phys. Chem. B* **2004**, *108*, 10256–10265.
(16) Terazono, Y.; Kodis, G.; Liddell, P. A.; Garg, V.; Gervaldo, M.; Moore, T. A.; Moore, A. L.; Gust, D. *Photochem. Photobiol.* **2007**, *83*, 464–469.
(17) Terazono, Y.; Kodis, G.; Liddell, P. A.; Garg, V.; Moore, T. A.; Moore, A. L.; Gust, D. *J. Phys. Chem. B* **2009**, *113*, 7147–7155.
(18) Cho, H. S.; Rhee, H.; Song, J. K.; Min, C.-K.; Takase, M.; Aratani, N.; Cho, S.; Osuka, A.; Joo, T.; Kim, D. *J. Am. Chem. Soc.* **2003**, *125*, 5849–5860.
(19) Barzilay, C. M.; Sibilia, S. A.; Spiro, T. G.; Gross, Z. *Chem.—Eur. J.* **1995**, *1*, 222–231.
(20) Almenningen, A.; Bastiansen, O.; Skancke, P. N. *Acta Chem. Scand.* **1958**, *12*, 1215–1220.
(21) Bart, J. C. J. *Acta Crystallogr., Sect. B* **1968**, *24*, 1277–1287.
(22) Larson, E. M.; Von Dreele, R. B.; Hanson, P.; Gust, D. *Acta Crystallogr.* **1990**, *C46*, 784–788.
(23) Förster, T. *Discuss. Faraday Soc.* **1959**, *27*, 7–17.
(24) Penzkofer, A.; Wiedmann, J. *Opt. Commun.* **1980**, *35*, 81–86.
(25) Hsiao, J.-S.; Krueger, B. P.; Wagner, R. W.; Johnson, T. E.; Delaney, J. K.; Mauzerall, D. C.; Fleming, G. R.; Lindsey, J. S.; Bocian, D. F.; Donohoe, R. J. *J. Am. Chem. Soc.* **1996**, *118*, 11181–11193.
(26) Gust, D.; Moore, T. A.; Moore, A. L. *Acc. Chem. Res.* **2009**, *42*, 1890–1898.
(27) Gust, D.; Moore, T. A.; Moore, A. L. *Acc. Chem. Res.* **2001**, *34*, 40–48.
(28) Wasielewski, M. R. *Chem. Rev.* **1992**, *92*, 435–461.